JOURNAL OF CATALYSIS 154, 33–40 (1995)

Pyridine Hydrodenitrogenation over Molybdenum Carbide Catalysts

Jeong-Gil Choi,* James R. Brenner,†,[1] and Levi T. Thompson†,[2]

*Department of Chemical Engineering, Han Nam University, Daejon 300-791, Korea; and †Department of Chemical Engineering, University of Michigan, Ann Arbor, Michigan 48109-2136

Received May 25, 1994; revised December 14, 1994

A series of molybdenum carbides was prepared by the temperature-programmed carburization of MoO_3 with pure CH_4 or an equimolar mixture of CH_4 and H_2. The resulting materials contained only Mo_2C in the bulk, but the surface areas and average pore sizes depended on the heating rate and H_2/CH_4 ratio employed. In general, the surface area increased with increases in the heating rate and/or H_2/CH_4 ratio. The Mo carbides were mesoporous with a small amount of microporosity and the average pore sizes ranged from 27 to 52 Å. Oxygen uptakes corresponded to ~13% of the Mo on the carbide surface being accessible. The Mo carbides were very active for pyridine hydrodenitrogenation with catalytic properties that were similar to those of Mo nitrides and superior to those of commercial sulfided Co–Mo and Ni–Mo/γ-Al_2O_3 hydrotreatment catalysts. Pyridine hydroenitrogenation over the Mo carbides appeared to be structure-sensitive as the activity and selectivity varied with changes in the surface area. Selectivities over the carbides were significantly different from those over the Mo nitride and sulfide catalysts. While the Mo carbides produced substantial amounts of cyclopentane, the Mo nitrides and the sulfided catalysts produced mostly pentane with only trace amounts of cyclopentane. These differences have been interpreted in terms of differing bonding geometries for pyridine on the Mo carbides and nitrides. © 1995 Academic Press, Inc.

1. INTRODUCTION

Hydrodenitrogenation (HDN) and hydrodesulfurization (HDS) are among the most important catalytic processes in converting crude oil and coal-derived liquids into clean-burning fuels. Nickel and/or Co promoted Mo sulfide catalysts are commonly used for these reactions. While Mo sulfide based catalysts are effective in meeting current industrial processing objectives, more stringent environmental pollution limits will require the development of new, more active, and selective catalysts. Molybdenum nitrides and carbides have shown great promise for use as commercial HDN (1, 2) and HDS (3, 4) catalysts. Recently we reported that the catalytic properties of unsupported (5) and supported (6) Mo nitrides were strong functions of their surface areas and loadings, respectively. These results encouraged our investigation of the effect of structure on the catalytic properties of Mo carbides. The purpose of the research described in this paper was to (i) systematically screen for the influence of the synthesis parameters including the heating rate, H_2/CH_4 ratio, and space velocity on the structural properties of Mo carbides prepared via the temperature-programmed carburization of MoO_3, and (ii) evaluate the pyridine HDN activities and selectivities of Mo carbides with a range of surface areas. A standard factorial design was used in this investigation along with the appropriate methods for analysis of the results.

2. EXPERIMENTAL

2.1. Synthesis

A series of unsupported Mo carbides was synthesized by the temperature-programmed carburization of MoO_3 (99.95%, Alfa, 0.9 m^2/g) with CH_4 (99.99%, Scott) or H_2/CH_4 mixtures. The heating rate, H_2 to CH_4 ratio, and CH_4 molar hourly space velocity were systematically varied in an effort to vary the carbide structural and compositional properties. A detailed description of the synthesis reactor system is given elsewhere (7).

Typically, between 1 and 6 g of MoO_3 powder was placed in the high temperature reactor on a quartz wool plug. The reaction temperature was quickly increased from room temperature to 823 K in 0.5 h. The temperature was then increased from 823 to 1093 K at 60 or 120 K/h and held at 1093 K for an additional hour. The molar hourly space velocity, defined as the ratio of the molar flow rate of CH_4 to the moles of MoO_3, was held constant at 10 or 30 h^{-1}. These synthesis conditions are similar to those employed previously to prepare Mo carbides (8, 9). After synthesis, the furnace was opened and the product was rapidly cooled to room temperature in the flowing

[1] Present address: Department of Chemistry, Argonne National Laboratories, Argonne, IL 60439.

[2] To whom correspondence should be addressed.

0021-9517/95 $6.00

reactant gas. Before exposure to air, the solid was purged with He for 10 min, then passivated for 2 h in a mixture of 0.996% O_2 in He (Scott) flowing at 20 cm^3/min. After passivation, the product was removed from the reactor for subsequent analysis.

2.2 Characterization

A Micromeritics ASAP 2000M sorption analyzer was used to determine the physisorption isotherms and pore size distributions. Prior to the analyses, the passivated materials were outgassed at 673 K for 5 h, then cooled to 77 K. The pore size distribution analysis was carried out using the software package supplied with the instrument. The BET surface area and O_2 chemisorption measurements were performed using a Quantasorb QS-17 sorption analyzer. Prior to the surface area measurements, the materials were pretreated isothermally under H_2 (20 cm^3/min) for 3 h at 673 K, purged for 10 min at 673 K in flowing He (20 cm^3/min), then cooled to room temperature. Single-point BET surface areas were determined using a mixture of 28.9% N_2 in He (Scott). Prior to measuring the O_2 uptakes, the carbides were reduced in flowing H_2 at 753 K for 3 h, then outgassed in flowing He at 753 K for ~15 minutes. Calibrated volumes of 5.11% O_2 in He (Scott) were injected into the He carrier gas passing over the catalyst until the surface was saturated. The volume of O_2 that was not adsorbed, was measured and used to determine the chemisorbed volume.

The bulk structures of the materials were evaluated using a computer-controlled Rigaku Rotaflex DMAX-B rotating anode diffractometer with a CuKα radiation source. The average crystallite sizes were estimated based on the peak-widths using the Scherrer formula (10). The peak-widths were corrected for instrumental broadening.

2.3. Reaction Rates and Product Distributions

The reaction rates and product distributions were measured under differential conditions (conversions less than 10%) using a 6.4 mm o.d. Pyrex glass flow reactor. Approximately 0.2 g of catalyst was loaded onto a plug of glass wool, and a thermocouple was inserted directly into the catalyst bed. The catalyst was heated under H_2 from room temperature to 773 K at a rate of 2 K/min, held at 773 K for at least 12 h, then cooled to the reaction temperature. The catalytic properties of two commercial hydrotreating catalysts, Crosfield 477 and 504 (Co–Mo and Ni–Mo supported on γ-Al_2O_3, respectively) were also evaluated. These catalysts were sulfided at 673 K in a mixture of 2% H_2S in H_2 for 4 h then reduced under H_2 at 673 K for ~12 h. These conditions are typical of those used to pretreat commercial hydrotreatment catalysts (11). The reaction rates were measured at temperatures between 588 and 638 K using 20 cm^3/min of flowing H_2 saturated with pyridine (99+%, Aldrich) at 273 K (0.61 kPa). The gaseous reactant mixture (total pressure of ~101 kPa) was passed over the catalyst, and the products were separated using a Hayesep D packed column and analyzed using a HP 5890 gas chromatograph equipped with a flame ionization detector.

3. RESULTS

3.1. Sorption Analysis

A typical N_2 adsorption and desorption isotherm set for an outgassed Mo carbide is given in Fig. 1. Isotherms of this nature are classified as Type IV according to guidelines set forth by Brunauer *et al.* (12) and the IUPAC (13). Type IV isotherms are common for materials containing mesopores (pore sizes between 20 and 500 Å). The hysteresis loop, which is associated with capillary condensation, is a Type B loop and indicated that the carbides contained slit-shaped pores created by aggregates of plate-like particles (14). Plots of the volume adsorbed versus the adsorbate film thickness (V–t curves) provide additional information about the nature of the pores. A typical V–t curve is shown in Fig. 2. The general character indicated that the carbides contained a small amount of micropores (pore sizes less than 20 Å) in addition to the mesopores. The behavior at small values of t corresponds to adsorption within the large pores and condensation in the micropores. There is a decrease in the slope of the line when the micropores are completely filled. Behavior at large values of t corresponds only to multilayer adsorption within the large pores. The sharpness of the transition between the two linear segments characterizes the size distribution for the micropores. There was a wide range of micropore sizes in most of the Mo carbides.

The Kelvin equation is commonly used to correlate the size to the pressure at which condensation occurs in a

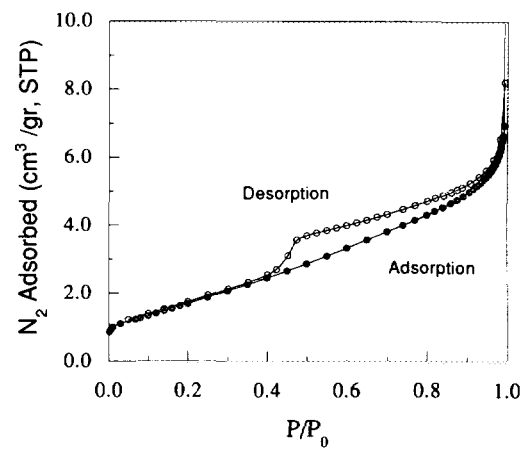

FIG. 1. Nitrogen adsorption and desorption isotherm set for MoC-6. These isotherms are typical of those of the other Mo carbides.

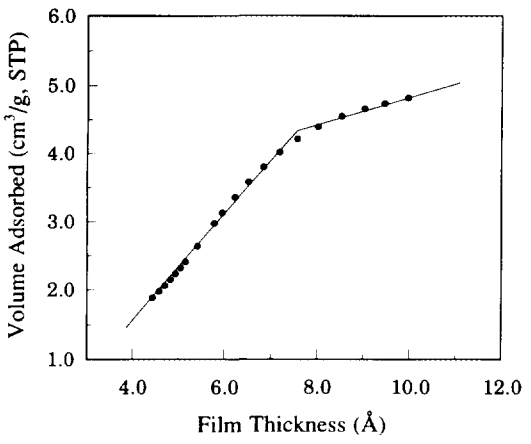

FIG. 2. The V–t curve for MoC-3. This curve is typical of the curves for the other Mo carbides.

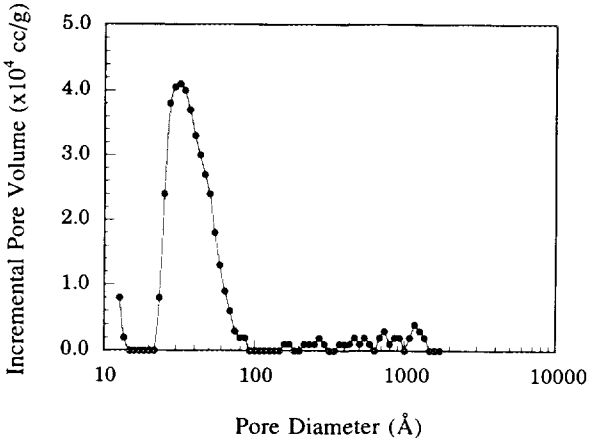

FIG. 3. The pore size distribution for MoC-4 determined based on the density functional theory model. The general character of this pore size distribution is typical of those of the other Mo carbides.

pore. We employed the Barrett–Joyner–Halenda (BJH) method, which is based on the Kelvin equation, for pore size distribution analysis. While the Kelvin equation may be regarded as exact for large pores, its accuracy decreases as the pore dimensions approach the micropore regime. Models based on density functional theory (DFT) are applicable for the entire range of pore sizes accessible by the adsorptive molecule, and approach those derived using the Kelvin equation at the large pore limit (15). Therefore, the Mo carbide pore size distributions were also evaluated based on density functional theory using the nitrogen on carbon with slit-like pores model. A typical pore size distribution is shown in Fig. 3. The Mo carbides had narrow pore size distrubitions, most of the pores being in the mesopore range (30–60 Å). Average pore sizes estimated from the DFT and BJH methods are compared in Table 1. The standard error in the average pore size was estimated to be ±14%. The average pore sizes calculated from the BJH method were larger than those determined from the DFT method. It is more common for pore size distributions derived using Kelvin-type models to underestimate the pore sizes; however, it is expected that the DFT method will yield more accurate meso- and micropore sizes.

The BET surface areas of the reduced Mo carbides ranged from 7 to 29 m^2/g depending on the synthesis conditions employed (see Table 1). These are similar to the surface areas reported elsewhere for hexagonal Mo_2C synthesized via the temperature-programmed carburization of MoO_3 (16). In general, the surface areas increased on increasing the heating rate and/or H_2/CH_4 ratio. The space velocity only had a small effect on the surface area over the range studied. Variations in the surface area with the heating rate and reactant gas composition were not surprising since these factors are expected to influence the solid-state reaction product selectivities (7). The presence of hydrogen in the feed mixture may have also suppressed the deposition of graphitic carbon thereby leaving

TABLE 1

Effect of Synthesis Parameters on Average Pore Sizes and Surface Areas

Catalyst code	Heating rate (K/h)	H_2/CH_4 ratio	CH_4 space velocity (h^{-1})	Average pore size (Å)		Surface area (m^2/g)
				DFT[a]	BJH[b]	
MoC-1	60	0	10	52	70	12
MoC-2	60	0	30	27	71	7
MoC-3	60	1.04	10	34	46	20
MoC-4	60	1.04	30	47	57	14
MoC-5	120	0	10	48	58	15
MoC-6	120	0	30	49	57	18
MoC-7	120	1.04	10	50	51	29
MoC-8	120	1.04	30	34	57	24

[a] Determined based on density functional theory model.
[b] Determined based on Barrett–Joyner–Halenda method.

TABLE 2

Chemisorptive Properties of the Molybdenum Carbides

Catalyst code	Surface area (m^2/g)	Oxygen uptake[a] ($\mu mol/g$)	Surface coverage ($\times 10^{14}$ O_2/cm^2)	Surface coverage (%)
MoC-1	12	12	0.60	11
MoC-2	7	9	0.80	15
MoC-3	20	24	0.72	13
MoC-4	14	11	0.49	9
MoC-5	15	23	0.92	17
MoC-6	18	—[b]		
MoC-7	29	36	0.75	14
MoC-8	24	19	0.48	9

[a] Measured at 195 K.
[b] Insufficient amount of material.

more of the carbide pore structure accessible. Thermodynamic considerations indicate that graphitic carbon would be produced at 450 K during the carburization of MoO_3 with pure CH_4 and at 800 K during carburization in an equimolar mixture of CH_4 and H_2 (8). The influence of the space velocity on surface area was not consistent with previous investigations in which the surface area increased with increasing space velocity for Mo carbides (1, 8) and Mo nitrides (1, 7). Variations in the surface area with the space velocity are usually attributed to the effects of gas phase products on the solid state reactions (7). It is possible that products formed during the carburization of MoO_3 were quickly swept away from the reaction interface even at the lowest space velocity employed.

Oxygen chemisorption provides a measure of the accessibility of the active surface (Table 2). Since atomic oxygen can diffuse into the subsurface layers of Mo carbides and nitrides (4, 17), the oxygen uptake was measured at 195 K. A straight line adequately represents the relationship between the O_2 uptake and BET surface area (Fig. 4). The slope of the line corresponds to a site density of 0.66×10^{14} O_2/cm^2. The density of the metal atoms on a clean carbide surface is 1.1×10^{15} Mo/cm^2, assuming that the surface consists of equal proportions of the low-index planes. The average oxygen uptake was therefore equivalent to an ~13% surface coverage by atomic oxygen or about one oxygen atom for every eight surface Mo atoms. The low uptake values may be due to the presence of graphitic carbon and/or oxygen residue from the synthesis at the surface. Oxygen, H_2, and CO do not chemisorb on graphitic carbon at 195 K (1, 18). Nevertheless, the O_2 uptake on the Mo carbides was of the same order of magnitude as that for O_2 chemisorption on Mo nitrides (16%) (5).

3.2. Bulk Properties

The only crystalline phase in the Mo carbides was Mo_2C. This observation was anticipated since according to the Mo–C phase diagram only hexagonal Mo_2C is thermodynamically stable under the conditions employed in this study (19). In the process of going from MoO_3 to Mo_2C, the specific volume decreased by 63%. This significant decrease in the specific volume would result in the generation of cracks, and the exposure of significant amounts of internal surface area. The Mo carbide crystallites were substantially smaller than those of the MoO_3 precursor and ranged from 50 to 200 Å based on the Mo_2C (101) reflection. The average particle sizes, estimated using

$$D_p = 6/S_g\rho, \qquad [1]$$

where S_g is the BET surface area and ρ is the density of the primary bulk phase, ranged from 200 to 1000 Å. The difference between the crystallite and particle sizes suggested the presence of polycrystalline aggregates. There was no correlation between the crystallite and particle sizes.

Texturing is typical for Mo nitrides prepared via the TPR of MoO_3 with NH_3 (20). We used the ratio of the intensities of the (002) and (101) reflections, $I(002)/I(101)$, as a measure of the texturing of the Mo_2C crystallites. The ratio for most of the materials was approximately 0.3, the value expected for randomly distributed Mo_2C crystallites of uniform dimensions (21). The only exception was MoC-4 for which $I(002)/I(101)$ was 0.7. This value indicated that crystallites in MoC-4 were not of uniform dimensions and/or were preferentially oriented. Both of these features may have been the consequence of the anisotropic nature of MoO_3. Molybdenum trioxide crystallites are typically elongated in the [010] direction.

3.3. Pyridine Hydrodenitrogenation

Selected Mo carbides were evaluated as pyridine hydrodenitrogenation catalysts. These materials were selected

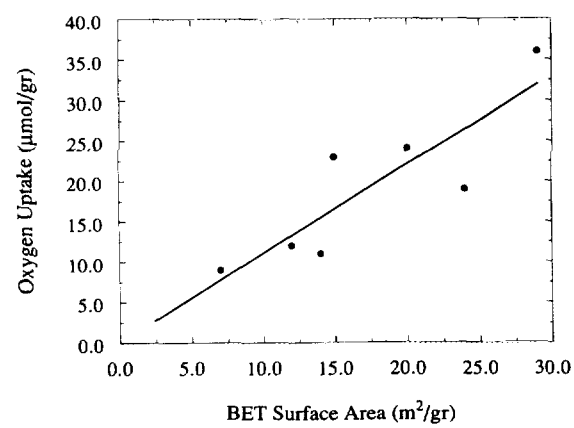

FIG. 4. A comparison of the BET surface areas and O_2 chemisorptive uptakes. The O_2 uptakes were measured at 195 K.

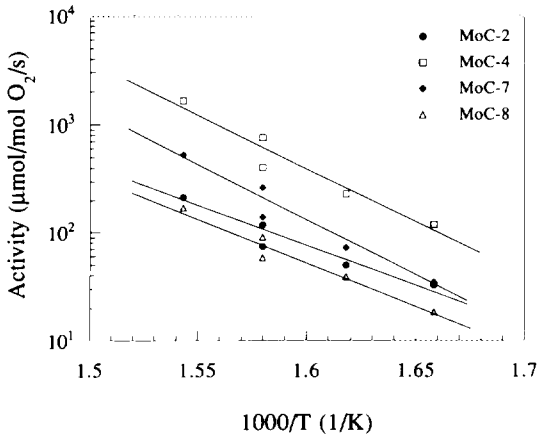

FIG. 5. Arrhenius plots of the pyridine HDN activities over selected Mo carbides. The surface areas of MoC-2, MoC-4, MoC-7, and MoC-8 were 7, 14, 29, and 24 m^2/g, respectively.

to span the entire range of surface areas produced. The activities decreased significantly prior to reaching steady state after ~100 min on stream; however, the product distributions were essentially unchanged. Figure 5 illustrates that over the temperature range studied, the steady state activities varied significantly with surface area. Note that MoC-4, the carbide that possessed crystallographic texturing, was the most active catalyst. These observations suggested that pyridine HDN was structure-sensitiveover the Mo carbides. Pyridine HDN (5) and thiophene HDS (4) have been reported to be structure-sensitive over Mo nitride catalysts. The HDN activities of the Mo carbides were compared to those of two unsupported Mo nitrides and two promoted Mo sulfide catalysts (Table 3). On an oxygen uptake basis, the carbides were in most cases less active than the nitrides; however, they were substantially more active than the Co–Mo and Ni–Mo sulfide catalysts. Apparent activation energies over the Mo carbides were similar or higher than those of the nitrides and sulfides. The activation energies for the sulfides were low but independent of the reactant flow rate, suggesting that transport limitations were not the cause.

Cyclopentane and pentane were the most abundant products for pyridine HDN over the carbides. Significant amounts of low-molecular weight hydrocarbons including methane were also produced. The C1–C4 hydrocarbons accounted for up to 35% of the product. The product distributions varied with surface area. The lower surface area carbides produced more cyclopentane than pentane, while the opposite was observed for the higher surface area materials. Product distributions for the Mo carbides were very different from those of the Mo nitride and sulfide catalysts (Fig. 6). While the Mo carbides produced significant amounts of cyclopentane, pentane was the most abundant product over the nitrides and sulfides. Only trace amounts of cyclopentane were produced over the Mo nitride and sulfided catalysts. These observations implied important differences between the catalytic sites on Mo carbides, nitrides, and sulfides.

4. DISCUSSION

The Mo carbides were as much as two orders of magnitude more active for pyridine HDN than sulfided Co–Mo/Al_2O_3 and Ni–Mo/Al_2O_3 hydrotreatment catalysts but activities of the Mo carbides were generally less than those of the Mo nitrides. Schlatter *et al.* (1) and Sajkowski and Oyama (22) also reported that Mo carbides are more active than promoted Mo sulfides; however, they found that the

TABLE 3

Summary of Pyridine Hydrodenitrogenation Results

Catalyst code	Surface area (m^2/g)	Reaction rate[a] (nmol/g/s)	Activity		ΔE_{act} (kcal/mol)
			(pmol/m^2/s)	(μmol/mol O_2/s)	
MoC-1	12	0.57	47	48	26
MoC-2	7	0.67	96	74	24
MoC-3	20	0.81	40	34	28
MoC-4	14	4.45	318	405	34
MoC-5	15	2.84	189	123	29
MoC-6	18	7.76	431	—	41
MoC-7	29	2.39	82	66	35
MoC-8	24	1.11	46	58	31
MoN-2[b]	116	46.7	403	362	25
MoN-8[b]	4	14.1	3535	2355	22
Co–Mo/Al_2O_3	—	0.17	—	.6	14
Ni–Mo/Al_2O_3	—	0.27	—	1.8	10

[a] Reaction rates measured at 633 K and ~101 kPa.

[b] The highest (MoN-2) and lowest (MoN-8) surface area Mo nitrides from Choi *et al.* [5].

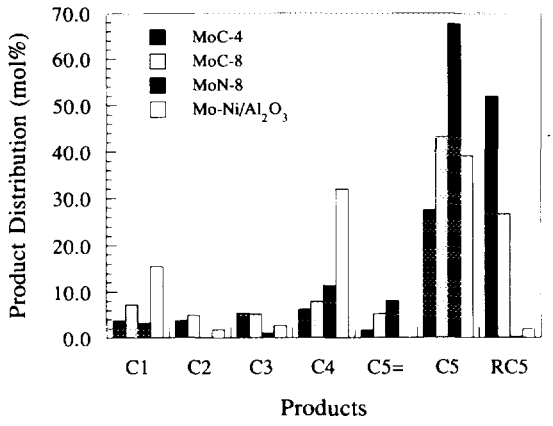

FIG. 6. A comparison of the pyridine HDN product distributions over the Mo carbide, Mo nitride, and sulfided Mo–Ni/Al_2O_3 catalysts. The selectivity measurements were made at 633 K and ~101 kPa. Cn represents an n-carbon hydrocarbon, C5= represents pentene and RC5 represents cyclopentane.

carbides were more active than the nitrides. This disparity is probably a consequence of the structure sensitivity of HDN over Mo carbides and nitrides.

The activities and product distributions for the Mo carbides were functions of their surface areas, suggesting that pyridine HDN over these materials was structure-sensitive. For metal catalysts structure sensitivity is associated with variations in the reaction rates with the crystallographic faceting of the surface (23). Surface faceting is a strong function of particle/crystallite size for domains smaller than 100 Å. Because Mo carbides are alloys, structure sensitivity should also include the influence of varying surface stoichiometries and structures. Recently we reported significant variations in the near surface compositions and structures for a series of Mo nitride catalysts with a range of surface areas (24). The bulk phase present in all of these materials was γ-Mo_2N (fcc), however, structures near the surface were body-centered with N/Mo ratios ranging from 0.48 to 1.3. It is possible that the surface compositions and structures for the Mo carbides also varied, resulting in significant variations in the catalytic properties. There is evidence that hydrogenolysis reactions are structure-sensitive over Mo carbides; however, except for this work there are no reports of structure sensitivity for HDN over Mo carbides. Lee *et al.* (25) reported that small α-MoC_{1-x} particles had higher butane hydrogenolysis activities than larger ones. In addition, the hydrogenolysis activity over Mo_2C was greater than that over α-MoC_{1-x} (fcc).

The Mo carbides produced significant amounts of cyclopentane, while pentane was the predominant product during pyridine HDN over the Mo nitrides and sulfides. These results indicated that reaction pathways available for the

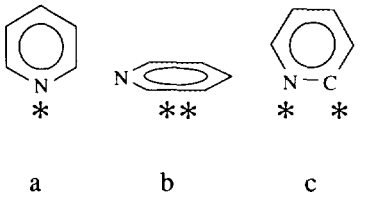

FIG. 7. Schematic illustrating the possible geometries for pyridine bonding to the active surface: (a) "end-on," (b) π-bound, and (c) α-pyridyllic. The asterisks represent bonding to a single site for * and multiple sites for **.

Mo carbides were different from those available for the nitrides and sulfides. It has been reported that Mo carbides show different selectivities than Mo nitrides during other hydrodenitrogenation and hydrodesulfurization reactions (1, 22). Differences observed in this work might be a consequence of differing pyridine bonding geometries. Armstrong *et al.* (26) reported that pyridine adsorbs onto Mo nitrides primarily through the nitrogen atom. This "end-on" bonding geometry would be amenable to the production of pentane via cleavage of the C–N bonds. While the end-on geometry could be used to rationalize pyridine product distributions for the Mo carbides, it is likely that a different bonding geometry is responsible. Plausible geometries include π-bound pyridine and α-pyridyl (Fig. 7). In both cases pyridine forms multiple bonds with the active surface. Multiply bonded intermediates have been proposed to explain product distributions during hydrodesulfurization over Mo sulfides (27). Multiple bonding might constrain pyridine in such a way as to keep the 2- and 6-position carbon atoms in close proximity. Given a sufficient residence time on the surface, it is possible that ring closure occurs producing cyclopentane. We propose a catalytic cycle of the form illustrated in Fig. 8 to account for the production of cyclopentane during pyridine HDN over the Mo carbides. The cyclopentane to pentane ratio varied with the surface area suggesting that the importance of this reaction pathway depended on the structure and/or composition of the carbide surface.

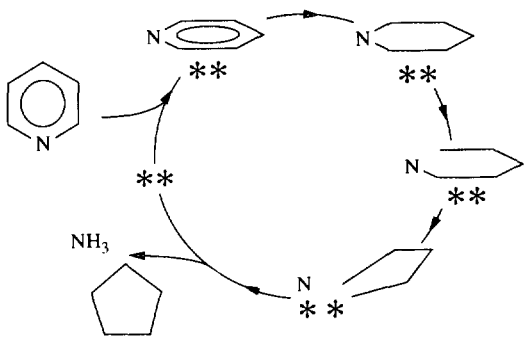

FIG. 8. Schematic illustrating a plausible catalytic cycle for the production of cyclopentane during pyridine HDN.

Differences in the bonding geometries of pyridine on the Mo carbides and nitrides might be understood in terms of the acid–base properties of the surfaces. Carbon and nitrogen are expected to have different effects on their associated Mo atoms. Electronegative elements like carbon have been reported to modify metal surface adsorption properties in a manner predicted by simple Lewis acid–base theory (28). Increasing the modifier electronegativity produces acid sites with acceptor orbitals that are lower in energy and geometrically more localized (29). Since nitrogen is more electronegative than carbon (30), Mo nitrides should be more acidic than Mo carbides. Ammonia temperature-programmed desorption results that will be reported in a future paper indicate that Mo nitride surfaces are more acidic than Mo carbide surfaces. One would expect the adsorption of pyridine, a Lewis base, to be stronger and more directional on Mo nitrides than on Mo carbides. This line of reasoning is consistent with the end-on adsorption of pyridine on Mo nitrides, and the more delocalized, perhaps multiple-site adsorption on Mo carbides.

5. CONCLUSIONS

Unsupported Mo carbides with a range of surface areas were prepared by the temperature-programmed carburization of MoO_3 with pure CH_4 or an equimolar mixture of CH_4 and H_2. In general, the materials contained Mo_2C in the bulk with no significant preferential orientation. The other structural properties of the materials were strong functions of the synthesis conditions employed. The most influential synthesis parameters were the heating rate and reactant gas composition. The highest heating rate and H_2/CH_4 ratio produced the highest surface area materials. The presence of H_2 in the feed mixture may have reduced the amount of carbon deposited on or in the materials thereby increasing the accessible surface area. The Mo carbides were mesoporous with average pore sizes ranging from 27 to 52 Å. These mesopores were slit-like, apparently as a consequence of the aggregation of plate-like particles. Most of the materials also contained a small amount of micropores.

The O_2 chemisorptive uptake varied linearly with the surface area suggesting that similar relative amounts of the Mo carbide surface were exposed in each of the materials. The results suggested that ~13% of the surface Mo atoms chemisorbed oxygen (assuming a Mo : O ratio of unity). This value is slightly less than that observed for O_2 chemisorption on Mo nitrides (16%).

The Mo carbides were active and selective for the hydrodenitrogenation of pyridine. Their activities were less than those of the Mo nitrides; however, the carbides were as much as two orders of magnitude more active than the Co- and Ni-promoted Mo sulfide catalysts. Pyridine hydrodenitrogenation over the Mo carbides appeared to be structure-sensitive since their activities and selectivities varied with changes in the surface area. This observation is consistent with our findings for the Mo nitrides. Product distributions for the Mo carbides were significantly different from those for the Mo nitride and sulfide catalysts. The carbides produced significant amounts of cyclopentane while the Mo nitrides and sulfides produced mostly pentane. We believe that these differences were due to differing pyridine bonding geometries with the active surface which gave rise to differing reaction pathways. The different bonding geometries may be a consequence of the different acid–base characteristics for Mo carbides and nitrides.

ACKNOWLEDGMENT

The authors acknowledge financial support from the National Science Foundation (CTS-9158527). We also thank Nedra Degraffenreid for assistance in determining the BET surface areas, and Sharath Franklin for the pore size measurements.

REFERENCES

1. Schlatter, J. C., Oyama, S. T., Metcalfe, J. E., and Lambert, J. M., *Ind. Eng. Chem. Res.* **27,** 1648 (1988).
2. Lee, K. S., Abe, H., Reimer, J. A., and Bell, A. T., *J. Catal.* **139,** 34 (1993).
3. Nagai, M., and Miyao, T., *Catal. Lett.* **15,** 105 (1992).
4. Markel, E. J., and Van Zee, J. W., *J. Catal.* **126,** 643 (1990).
5. Choi, J.-G., Brenner, J. R., Colling, C. W., Demczyk, B. G., Dunning, J., and Thompson, L. T., *Catal. Today* **15,** 201 (1992).
6. Colling, C. W., and Thompson, L. T., *J. Catal.* **146,** 193 (1994).
7. Choi, J.-G., Curl, R. L., and Thompson, L. T., *J. Catal.* **146,** 218 (1994).
8. Lee, J. S., Oyama, S. T., and Boudart, M., *J. Catal.* **106,** 125 (1987).
9. Volpe, L., and Boudart, M., *J. Solid State Chem.* **59,** 348 (1985).
10. Cullity, B. D., "Elements of X-ray Diffraction," p. 102. Addison–Wesley, MA, 1978.
11. Katzer, J. R., and Sivasubramian, R., *Cat. Rev.-Sci. Eng.* **20**(2), 155 (1979).
12. Brunauer, S., Demming,L. S., Demming, W. S.,and Teller, E., *J. Am. Chem. Soc.* **62,** 1723 (1940).
13. Sing, K. S. W., Everett, D. H., Haul, R. A. W., Moscou, L., Pierotti, R. A., Roulqûerol, J., and Siemieniewska, T., *Pure Appl. Chem.* **57**(4), 603 (1985).
14. De Boer, J. H., *in* "The Structure and Properties of Porous Materials" D. H. Everett, and F. S. Stone, Eds.), p. 68. Butterworth, London (1958).
15. Seaton, N., Walton, J. P. R. B., and Quirke, N., *Carbon* **27,** 853 (1989).
16. Leciercq, L., Imura, K., Yoshida, S., Barbee, T., and Boudart, M., *in* "Preparation of Catalysts II" (B. Delmon, Ed.), p.627. Elsevier, New York, (1978).
17. Leary, K. J., Michaels, J. N., and Stacy, A. M., *J. Catal.* **101,** 301 (1986).
18. Boudart, M., *J. Catal.* **103,** 30 (1987).
19. Rudy, E., Windisch, S., Stosick, A. J., and Hoffman, J. R., *Trans. TMS-AIME* **239,** 1247 (1967).
20. Boudart, M., and Volpe, L., *J. Solid State Chem.* **59,** 332 (1985).

21. McClune, W. F., (Ed.), "Powder Diffraction File; Alphabetical Index Inorganic Materials," International Centre for Diffraction Data, Swarthmore, PA, (1991).
22. Sajkowski, D. J., and Oyama, S. T., *in* "Symposium on The Chemistry of W/Mo Catalysis, 199th ACS National Meeting, Boston, MA, April 22–27, 1990," *Prepr. Am. Chem. Soc. Div. Pet. Chem.* **35**(2), 233 (1990).
23. Boudart, M., and Djega-Mariadassou, G., "Kinetics of Heterogeneous Catalytic Reactions," p. 155. Princeton Univ. Press, Princeton, NJ, (1984).
24. Demczyk, B. G., Choi, J.-G., and Thompson, L. T., *Appl. Surf. Sci.* **78,** 63 (1994).
25. Lee, J. S., Locatelli, S., Oyama, S. T., and Boudart, M., *J. Catal.* **125,** 157 (1990).
26. Armstrong, P. A., Bell, A. T., and Reimer, J. A., *J. Phys. Chem.* **97,** 1952 (1993).
27. Cowley, S. W., Ph.D. Dissertation, Southern Illinois University, 1975.
28. Stair, P. C., *J. Am. Chem. Soc.* **104,** 4044 (1982).
29. Deffeyes, J. E., Horlacher Smith, A., and Stair, P. C., *Appl. Surf. Sci.* **26,** 517 (1986).
30. Huheey, J. E., "Inorganic Chemistry; Principles of Structure and Reactivity," p. 168. Harper & Row, New York, (1978).